

LOW-VOLTAGE LATERAL-CONTACT MICRORELAYS FOR RF APPLICATIONS

Ye Wang¹, Zhihong Li², Daniel T. McCormick¹ and Norman C. Tien

Berkeley Sensor and Actuator Center, Department of Electrical and Computer Engineering,
University of California at Davis, Davis, CA 95616

¹also at Department of Electrical and Computer Engineering, Cornell University, Ithaca, NY 14853

²also at Institute of Microelectronics, Peking University, Beijing, China

Email: yw51@cornell.edu

ABSTRACT

This paper reports the design and fabrication of a low-voltage lateral-contact microrelay for RF applications. The silicon surface micromachined relay utilizes electro-thermal actuators and low-stress silicon nitride as a structural connection as well as electrical and thermal isolation. The sidewall contact is sputtered gold. The driving voltage is measured to be as low as 8V. RF testing shows that the microrelay has an off-state isolation of -20dB at 12GHz. The simplicity of this four-mask fabrication process enables the possible integration with other RF MEMS components.

INTRODUCTION

With the recent progress of MicroElectroMechanical System (MEMS) technology, more and more attention has been focused on the development of MEMS devices for RF applications. MEMS switches are one of the most promising future micromachined products that have attracted numerous research efforts in recent years. They have many potential applications including signal routing in RF system front-ends, impedance matching networks, filter-path selection circuits and other high-frequency reconfigurable circuit applications. Compared to their conventional electromechanical or solid-state counterparts, micromachined relays offer many advantages in terms of low insertion loss, high off-state isolation and linearity, high breakdown voltage and integration capability. The majority of the reported MEMS switches employs electrostatic actuation [1-4] and operates with large actuation voltage. Few are lateral relays [5-6] and those often require non-standard post process and they are only suitable for DC applications. Some of the conventional parallel-plate MEMS switches have limited RF performance due to loss caused by capacitive coupling between the contacting bar and the substrate at high frequency. An adequate closing gap to achieve high isolation usually results in a large actuation voltage. In addition, the signal line and the contacting bar have to be realized by two separate process steps.

We present a lateral-contact microrelay fabricated on a silicon substrate using surface micromachining technology. This relay is electro-thermally actuated and

exhibits high RF performance due to its lateral contact mechanism. The microrelay consists of polysilicon and low-stress silicon nitride as structural materials and sputtered gold as the contact metal. Metal contact is realized by in-plane motion and sidewall connection.

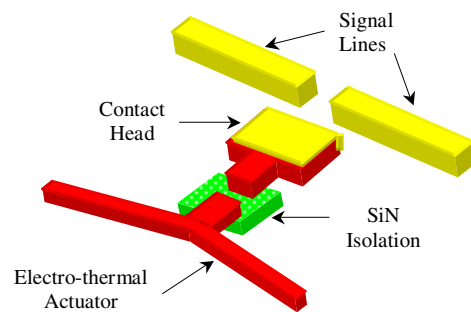


Figure 1. Schematic illustration of the microrelay.

DESIGN

Figure 1 illustrates the operation principle of the microrelay. It utilizes electro-thermal actuators, for which extensive research has been done both theoretically and experimentally [7-8]. The thermal expansion caused by current flowing through a V-shaped beam actuates the contact head through silicon nitride connection. The resulting in-plane motion of the contact head allows it to move forward and connect the RF signal lines via sidewall contact.

V-shaped actuator beams were chosen for their rectilinear displacements caused by resistive heating and their large output force in the range of millinewtons [7]. This will provide a stable contact with low contact resistance in the range of milliohms [9]. Actuator beams of the same dimension are cascaded to produce larger displacement, as depicted in Figure 2. A current flow between terminal A and B will cause all three V-beams to expand due to resistive heating. The thermal expansion of the two side beams increases the vertical displacement of the central beam. This generates a larger deflection at the tip compared to a single actuator beam.

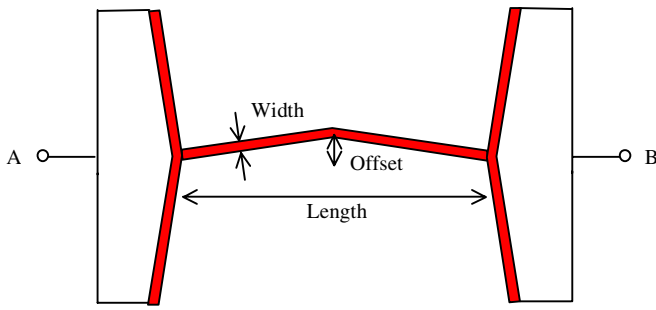


Figure 2. Schematics of the cascaded thermal actuator beams (top view).

The nominal dimension of a single actuator beam has a length of $200\mu\text{m}$, width and thickness of $2\mu\text{m}$ and center offset of $10\mu\text{m}$. The actuator beam with this design value is calculated to have a high shock resistance $> 5000g$ ($g = 9.8\text{m/s}^2$) and self-resonance frequency of 31.9kHz , which indicates good mechanical robustness. The microrelay itself occupies an area of $200 \times 220\mu\text{m}^2$ if not considering the RF testing pad. Test structures of cascaded actuator beams with various dimensions were designed and simulated. Table 1 shows the design values and ANSYS simulation of their displacements under a given thermal load. Type 1 design gives the nominal dimensions.

Table 1. Various actuator test structures and their simulated displacements.

	Length	Width	Offset	Disp.
Type1	$200\mu\text{m}$	$2\mu\text{m}$	$10\mu\text{m}$	$5.4\mu\text{m}$
Type2	$240\mu\text{m}$	$2\mu\text{m}$	$10\mu\text{m}$	$7.2\mu\text{m}$
Type3	$240\mu\text{m}$	$1\mu\text{m}$	$15\mu\text{m}$	$6.2\mu\text{m}$
Type4	$260\mu\text{m}$	$1.5\mu\text{m}$	$10\mu\text{m}$	$7.9\mu\text{m}$
Type5	$280\mu\text{m}$	$2\mu\text{m}$	$10\mu\text{m}$	$8.6\mu\text{m}$
Type6	$300\mu\text{m}$	$2\mu\text{m}$	$15\mu\text{m}$	$9.2\mu\text{m}$

Gold is chosen as contact metal because of its low resistivity, good stability and efficiency in RF signal propagation. It has a skin depth of $0.71\mu\text{m}$ at 12GHz and $0.45\mu\text{m}$ at 30GHz . Thickness of $0.5\mu\text{m}$ is used due to sputtering limit. Sputtered gold is known to have higher hardness which gives less surface damage for metallic microcontacts [9].

Different contact head shapes including round, square and angled have been designed to explore their reliabilities. Contact head areas between $700\mu\text{m}^2$ to $1200\mu\text{m}^2$ are designed after considering the tradeoff between contact resistance and the load the contact head puts on the extension beams. The closing gap between the contact head and the signal lines is between $3\text{--}5\mu\text{m}$ to ensure good sidewall coverage of the sputtered gold in the trench.

FABRICATION

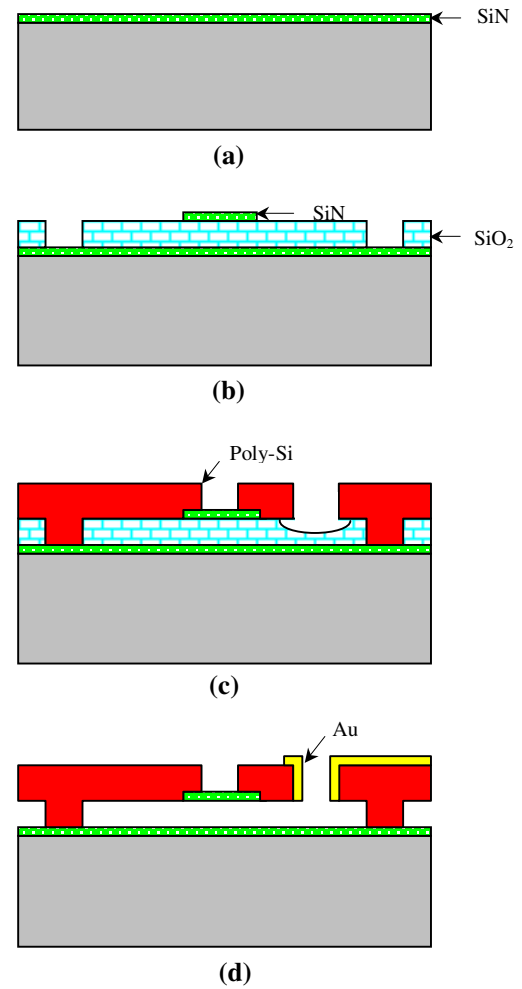


Figure 3. Schematic of the process flow: (a) deposition of the low-stress SiN as isolation; (b) deposition and patterning of sacrificial SiO₂ and low-stress SiN connection; (c) deposition and patterning of poly-Si and partial release; (d) Sputtering and lift-off of Au and HF release.

The fabrication process is depicted in Figure 3. First, $0.6\mu\text{m}$ of Low-Pressure Chemical-Vapor-Deposited (LPCVD) low-stress silicon nitride is deposited at temperature of 850°C . It is used as an isolation layer to reduce substrate loss. Then $2\mu\text{m}$ of sacrificial oxide is deposited and anchors are patterned. Afterwards another $0.6\mu\text{m}$ of LPCVD low-stress silicon nitride is deposited and patterned. It serves as the structural connection as well as the electrical and thermal isolation between the driving structure and the contact structure. Figure 4 (a) is the SEM micrograph of a piece of silicon nitride connecting two polysilicon structures; no stress mismatch between the two materials was observed. A few different structural connections are designed to explore the possibilities, as shown in Figure 4 (b). Next $2\mu\text{m}$ of *in situ*

doped n-type polysilicon film is deposited at 620°C. It is patterned using 0.4µm oxide as hard mask. A partial release step is then performed at the closing gap region to ensure the separation of sputtered gold on the contact head sidewall and the signal lines, as well as the removal of unwanted gold in the area between them.

In the next step, a thin layer of gold (0.3-0.5µm) is sputtered and lifted off, leaving gold only on the contact sidewalls and signal routing lines. Figure 5 shows a uniform coverage of gold on the contact sidewalls. The warpage on the edge of the signal line is due to lift-off. Finally, the device is released in hydrofluoric acid and the polysilicon and silicon nitride structures are suspended above the substrate. A supercritical CO₂ drying after HF release is helpful to reduce the surface stiction of the thin actuator beams.

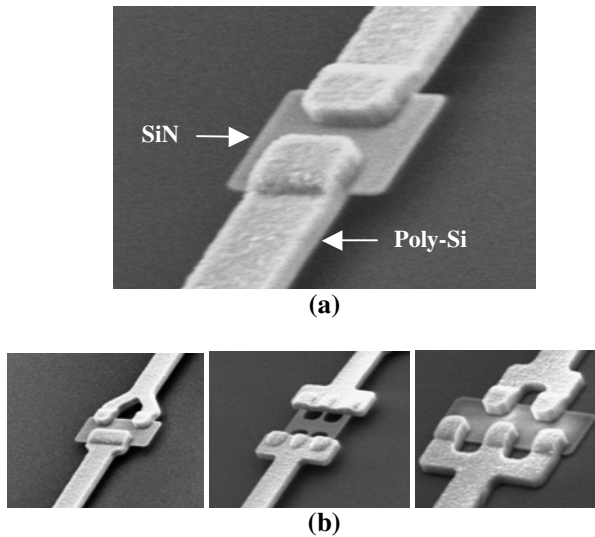


Figure 4. (a) SEM image of the SiN structure connecting two polysilicon structures; (b) SEM images of different structural connections.

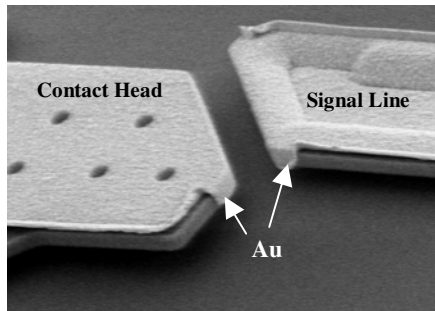


Figure 5. SEM image of the contact sidewalls and signal line coated with gold.

The fabrication is completed using standard MEMS processes with only four masks, including lift-off, and no

post-processing is required. Contact metal is realized using one-step gold sputtering. The simplicity of this process allows design flexibility, and possible integration of this microrelay with other passive RF MEMS components.

RESULTS AND DISCUSSIONS

Electrical testing was done with an HP 4145B Parameter Analyzer at room temperature in an air ambient environment. It shows the microrelay can be operated at voltages of 8-15V with contact resistance less than 1Ω. The operating voltage can be further reduced by decreasing the closing gap between the contact head and the signal lines or using highly doped polysilicon. Contact heads with round and square shape showed better reliability than the angled-shape contact heads.

During the microrelay on-state, the power consumption of the thermal actuator is in the range of 20-40mW. The break down voltage of the signal path is measured to be as high as 500V.

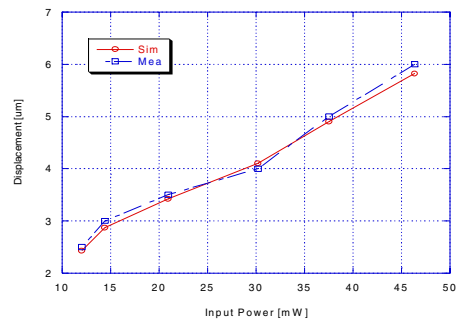


Figure 6. Measured actuator displacement vs. simulated values at various input power.

The measured actuation displacements at different input power for the actuator beam arrays with nominal dimension were plotted in Figure 6. Simulation parameters were adjusted to account for their changes due to thermal heating. This gives good agreement between the measured displacement and simulation, which shows a linear proportion to the input power. Test structures listed in Table 1 were tested and their actuation distances were compared with ANSYS simulations. Theoretical calculation [7-8] is also used to verify the results.

RF testing was performed using an HP8510C network analyzer and coplanar ground-signal-ground (GSG) probes with 150µm pitch. Two-port S-parameters were measured and parasitics of the testing pads were de-embedded. Figure 7 shows the measured off-state isolation is -20dB at 12GHz. The measurements also indicate the microrelay has an insertion loss of less than -1dB at 12GHz with most resistive loss occurs on the signal lines.

A comparison between some of the most recent microrelays and this design is tabulated in Table 2. It shows that the microrelay exhibits high isolation in the GHz frequency range comparable to those fabricated on GaAs substrate with similar actuation voltage.

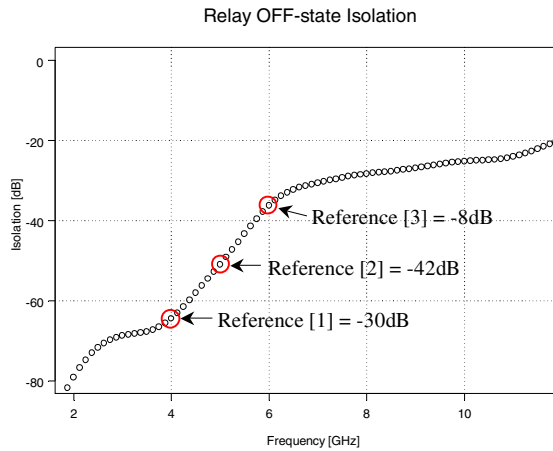


Figure 7. Measured relay off-state isolation.

Table 2. Comparison of selected recent MEMS relays and this design.

Ref.	Motion	Substrate	Voltage	Isolation
[1]	Vertical	GaAs	5V	-30dB@4GHz
[2]	Vertical	GaAs	8V	-42dB@5GHz
[3]	Vertical	Si	10V	-8dB@6GHz
[4]	Vertical	GaAs	70V	-30dB@40GHz
This Design	Lateral	Si	8V	-20dB@12GHz

Reliability study of the microrelay shows that metal contact welding causes the most failures. Surface roughness on the sidewall may also result in bad contacts. The high adherence force of gold plays a role in the contact degradation as well. Gold and Nickel alloy can be considered as an alternative choice of contact metal due to its small adherence force and relatively low resistivity.

CONCLUSION

An electro-thermally actuated lateral-contact microrelay for RF applications has been designed and fabricated on silicon substrate using surface micromachining technology. Low-stress silicon nitride as structural connection shows promising results with good electrical isolation and negligible stress mismatch. The lowest actuation voltage of the microrelay is 8V. The microrelay has an off-state isolation of -20dB at 12GHz and low insertion loss of less than -1dB. The lateral contact mechanism of the microrelay provides a high RF performance. The measured off-state isolation in the GHz

frequency range is comparable with some recently reported RF MEMS switches fabricated on semi-insulating substrate. The simplicity of the fabrication process enables the possible integration of the microrelay with other passive RF MEMS components.

ACKNOWLEDGEMENTS

The authors would like to thank Prof. Edwin Kan for providing the testing equipment and the staff of Cornell Nanofabrication Facility. The authors would also like to thank A. Yeh, H. Jiang, K. Yoo and Z. Liu for their fruitful discussions.

REFERENCES

- [1] D. Hah, E. Yoon and S. Hong, "A Low-Voltage Actuated Micromachined Microwave Switch Using Torsion Springs and Leverage", *IEEE Trans. Microwave Theory and Techniques*, Vol. 48, No. 12, pp. 2540-2545, Dec. 2000
- [2] J. Y. Park, G. H. Kim, K. W. Chung and J. U. Bu, "Electroplated RF MEMS Capacitive Switches", *Proc. IEEE/ASME Int. Conference on Micro Electro Mechanical Systems (MEMS 2000)*, Interlaken, Switzerland, pp. 639-644, Jan. 2000
- [3] F. Plotz, S. Michaelis, G. Fattinger, R. Aigner and R. Noe, "Performance and Dynamics of a RF MEMS Switch", *Proc. IEEE Int. Conference on Solid-State Sensors and Actuators (Transducers '01)*, Munich, Germany, pp. 1560-1563, June 2001
- [4] R. E. Mihailovich, M. Kim, J. B. Hacker, E. A. Sovero, J. Studer, J. A. Higgins and J. F. deNatale, "MEM Relay for Reconfigurable RF Circuits", *IEEE Microwave and Wireless Components Letters*, Vol. 11, No. 2, pp. 53-55, Feb. 2001
- [5] E. J. J. Kruglick and K. S. J. Pister, "Lateral MEMS Microcontact Considerations", *IEEE J. Microelectromechanical Systems*, Vol. 8, No. 3, pp. 264-271, Sept. 1999
- [6] J. Simon, S. Saffer, F. Sherman and C.-J. Kim, "Lateral Polysilicon Microrelays with a Mercury Microdrop Contact", *IEEE Trans. Industrial Electronics*, Vol. 45, No. 6, pp. 854-860, Dec. 1998
- [7] L. Que, J.-S. Park and Y. B. Gianchandani, "Bent-Beam Electrothermal Actuators-Part I: Single Beam and Cascaded Devices", *IEEE J. Microelectromechanical Systems*, Vol. 10, No. 2, pp. 247-262, June 2001
- [8] J. M. Maloney, D. L. DeVoe and D. S. Schreiber, "Analysis and Design of Electrothermal Actuators Fabricated From Single Crystal Silicon", *Proc. ASME Int. Mechanical Engineering Congress and Exposition*, pp. 233-240, May 2000
- [9] D. Hyman and M. Mehregany, "Contact Physics of Gold Microcontacts for MEMS Switches", *IEEE Trans. Components and Packaging Technology*, Vol. 22, No. 3, pp. 357-364, Sept. 1999